Synthesis of highly stable red-emissive carbon polymer dots by modulated polymerization: from mechanism to application in intracellular pH imaging

Jie Xia,[a] Shuai Chen,[b] Guang-Yue Zou,[a] Yong-Liang Yu*[a] and Jian-Hua Wang[a]

[a]*Research Center for Analytical Sciences, Department of Chemistry, College of Sciences, Northeastern University, Box 332, Shenyang 110819, China*

[b]*College of Life and Health Sciences, Northeastern University, Shenyang 110169, China.*

*Corresponding author.

E-mail: yuyl@mail.neu.edu.cn (Y.-L. Yu)

Tel: +86 24 83688944; Fax: +86 24 83676698

Electronic Supplementary Information

Materials

p-Phenylenediamine (pPD) was purchased from Sinopharm Chemical Reagent Co., Ltd. (Shanghai, China). $FeCl_3 \cdot 6H_2O$ and 4-(2-hydroxyethyl)-1-piperazineethanesulfonic acid (HEPES) were purchased from Aladdin Chemistry Co., Ltd. (Shanghai, China). 3-(4,5-Dimethylthiazol-2-yl)-2,5-diphenyl-2H-tetrazolium (MTT) was purchased from Dalian Meilun Biotechnology Co., Ltd. (Dalian, China). Nigericin was purchased from Toronto Research Chemicals Inc. (North York, Canada). Dexamethasone (DEX) was purchased from Sigma-Aldrich LLC. (USA). All reagents were used as received without further purification. Ultrapure water (18 MΩ cm) was used throughout the experiments. 10 mM pPD and 100 mM $FeCl_3$ aqueous solutions were prepared and stocked at 4°C for further use. The Britton-Robinson (BR) buffer was prepared by mixing 40 mM acetic acid, boric acid, and phosphoric acid. The pH was adjusted by different amounts of 1 M NaOH or HCl solution.

Instrumentations

Transmission electron microscopy (TEM) observations were performed on a Tecnai $G^2$20 transmission electron microscope (FEI, USA). High-resolution TEM (HRTEM) images were obtained with a JEM 2100F transmission electron microscope (JEOL, Japan). Atomic force microscopy (AFM) images were recorded by using a DIMENSION ICON atomic force microscope (Bruker, Germany). X-ray diffraction (XRD) patterns were collected on an Empyrean powder X-ray diffractometer (PANalytical B.V., Holland) with Cu Kα radiation at λ 1.54Å. Fluorescence (FL) spectra were recorded on an F-7000 FL spectrophotometer (Hitachi High-Technologies, Japan). Ultraviolet-visible (UV-vis) absorption spectra were recorded on a U-3900 spectrophotometer (Hitachi High-Technologies, Japan). Quantum yields were measured on a C11347 absolute photoluminescence (PL) quantum yield spectrometer (Hamamatsu Photonic K.K., Japan). Fourier transform infrared (FT-IR) spectra were recorded on a Nicolet-6700 spectrophotometer (Thermo Instruments Inc., USA). X-ray photoelectron spectroscopy (XPS) scanning curves were obtained on an ESCALAB 250XI surface analysis system with Al/Kα as the source (Thermo Electron Corporation, USA). HeLa cells were cultured in a HERA Cell 150 incubator (Thermo Instruments Inc., USA). MTT assay was conducted by using a Synergy H1 ELISA plate reader at 570 nm (BioTek Instruments Inc., USA). Confocal laser scanning microscope (CLSM) images were obtained on a FV 1200 CLSM (transmissivity of 488 nm laser: 75%, PMT voltage: 750 V, C.A.: 95 μm) (Olympus Corporation, Japan).

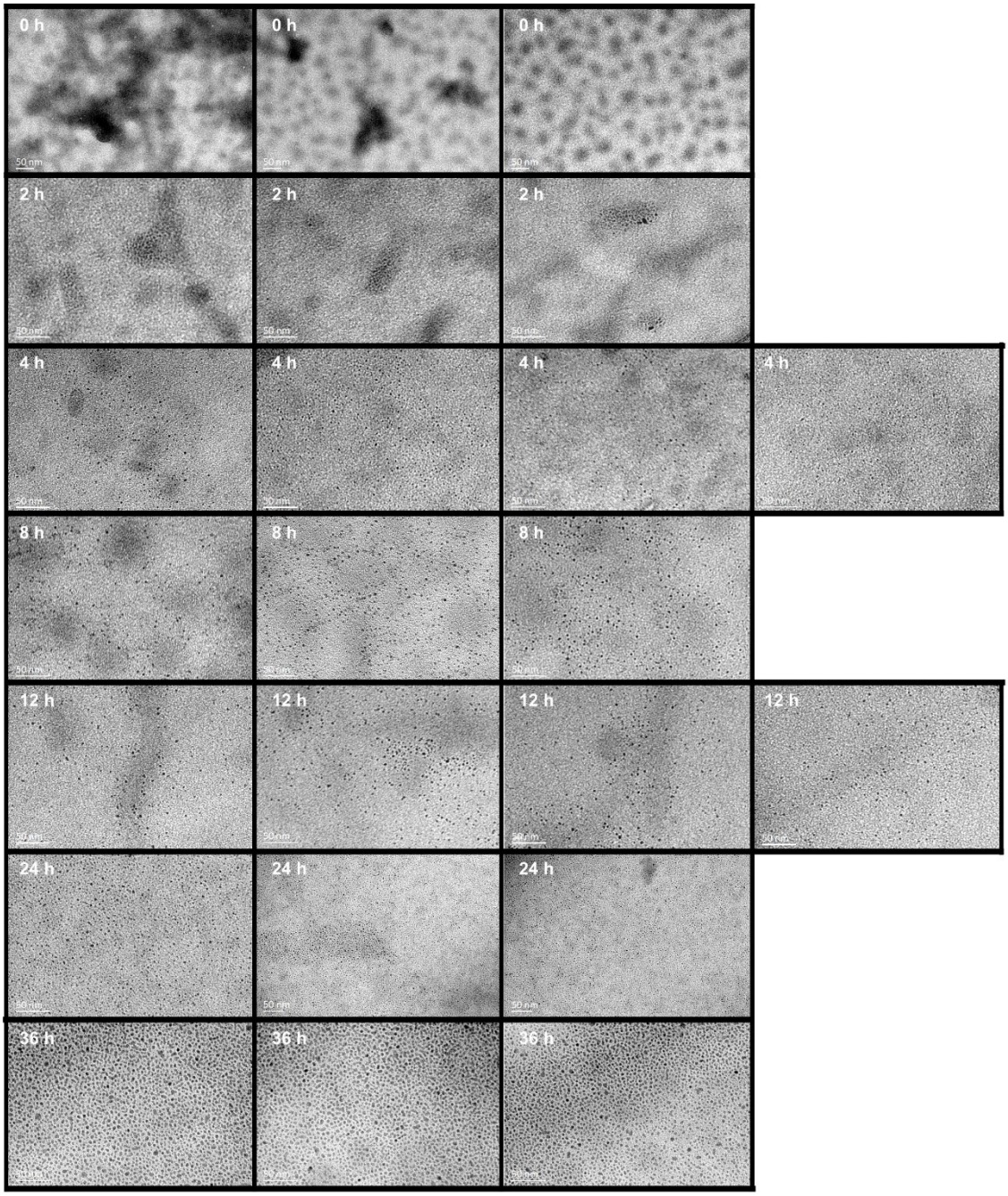

Fig. S1 TEM images of the R-CPDs at different heating durations.

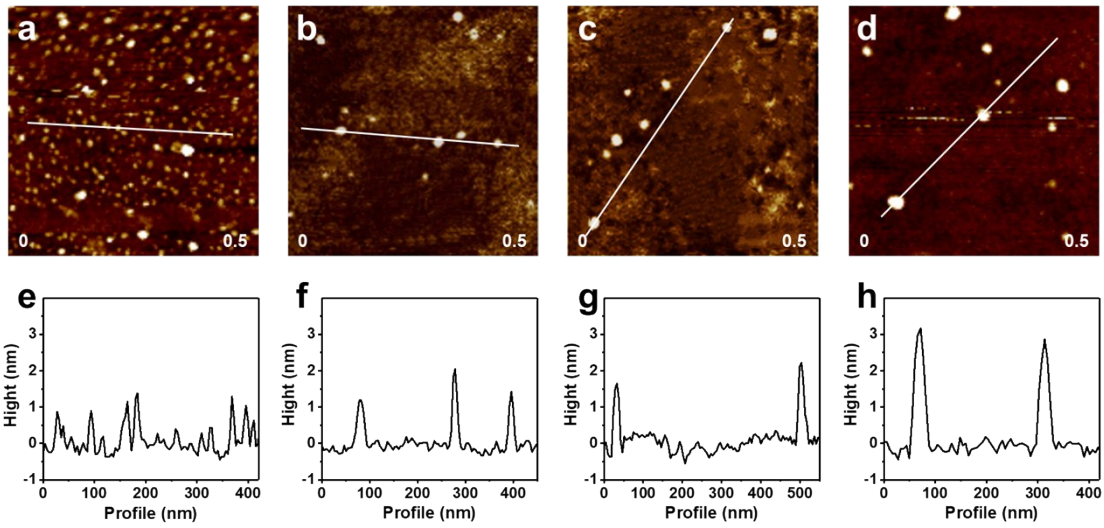

Fig. S2 AFM images and corresponding height profiles of the R-CPDs at different heating durations of (a, e) 2 h, (b, f) 12 h, (c, g) 24 h and (d, h) 36 h.

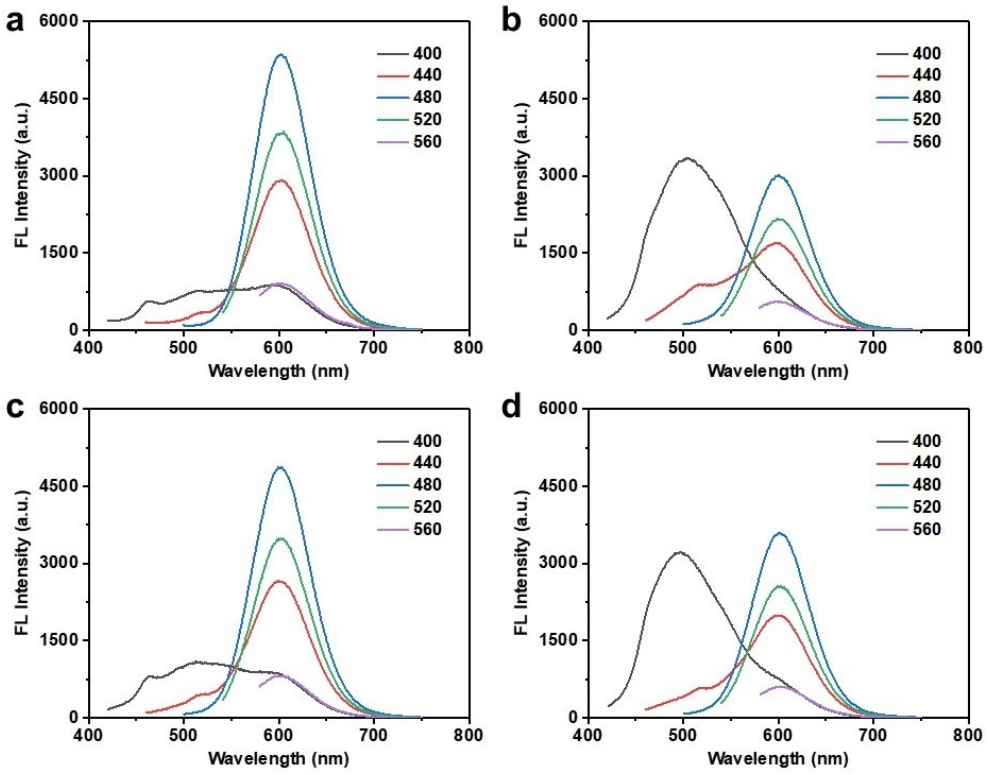

Fig. S3 FL spectra of the R-CPDs obtained by heating reaction for 12 h in the presence of 50 μM (a) $FeCl_3$, (b) $CuCl_2$, (c) $Fe(NO_3)_3$ and (d) $AgNO_3$, respectively. Other conditions: 1 mM pPD, temperature: 80°C, pH=7.

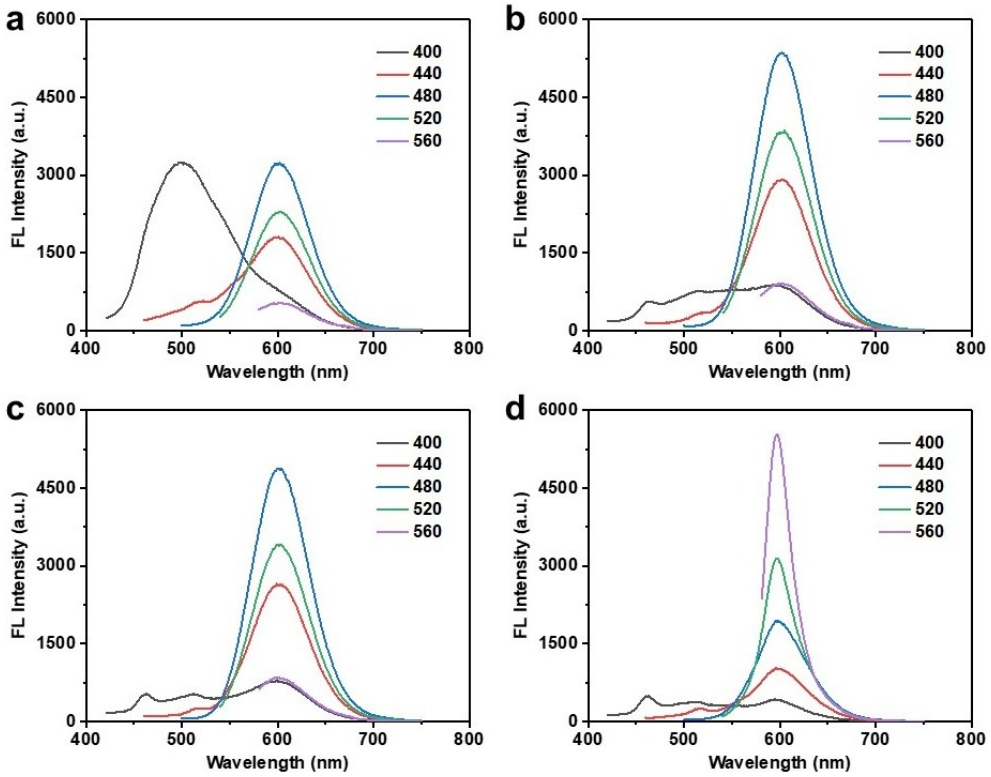

Fig. S4 FL spectra of the R-CPDs obtained by heating reaction for 12 h in the presence of (a) 0, (b) 50, (c) 100 and (d) 200 μM $FeCl_3$, respectively. Other conditions: 1 mM pPD, temperature: 80°C, pH=7.

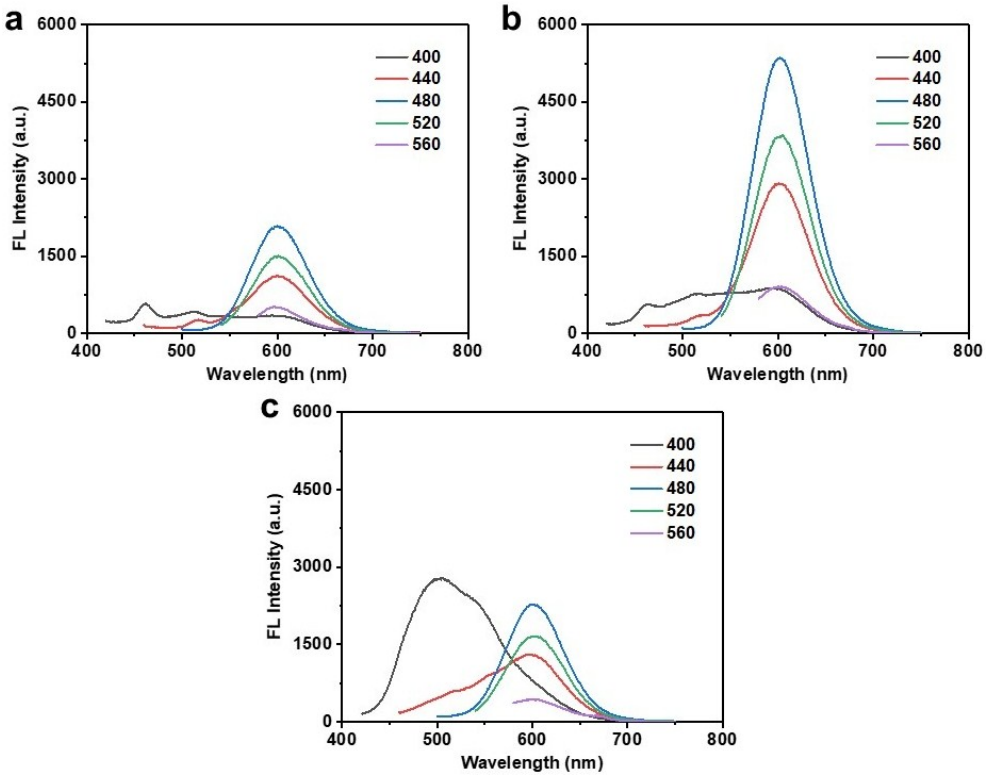

Fig. S5 FL spectra of the R-CPDs obtained by heating reaction for 12 h with (a) 0.2, (b) 1.0 and (c) 5.0 mM pPD, respectively. Other conditions: 50 μM $FeCl_3$, temperature: 80°C, pH=7.

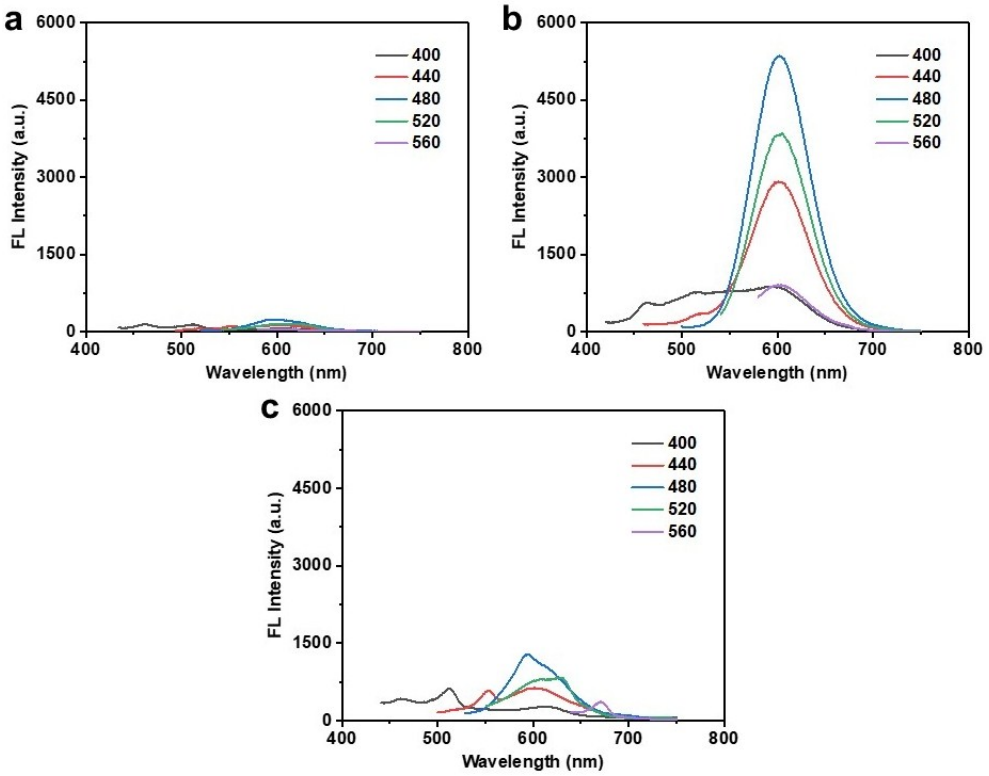

Fig. S6 FL spectra of the R-CPDs obtained by heating reaction for 12 h at (a) 40, (b) 80 and (c) 120°C, respectively. Other conditions: 1 mM pPD, 50 μM $FeCl_3$, pH=7.

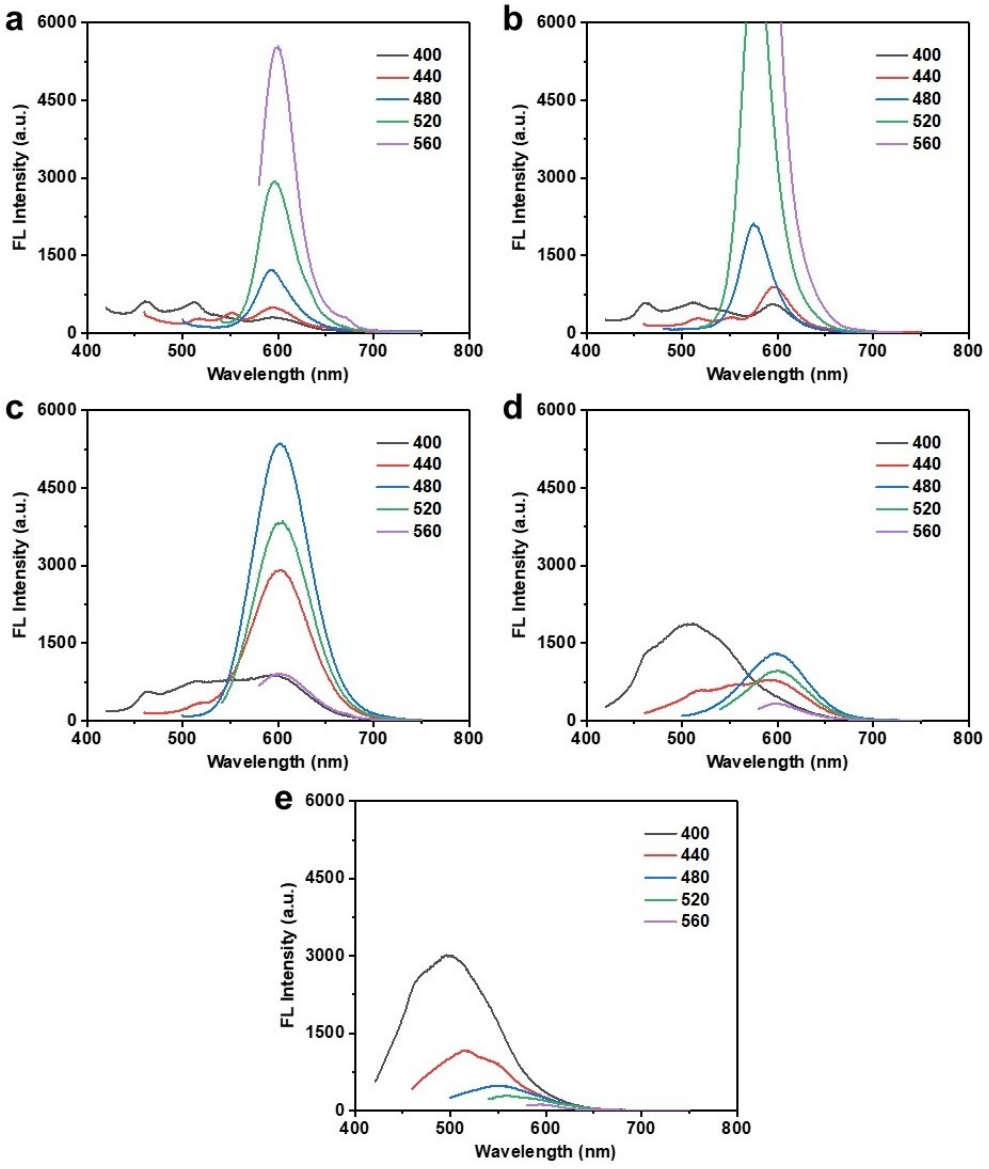

Fig. S7 FL spectra of the R-CPDs obtained by heating reaction for 12 h at initial pH of (a) 3, (b) 5, (c) 7, (d) 9 and (e) 11, respectively. Other conditions: 1 mM pPD, 50 μM $FeCl_3$, temperature: 80°C.

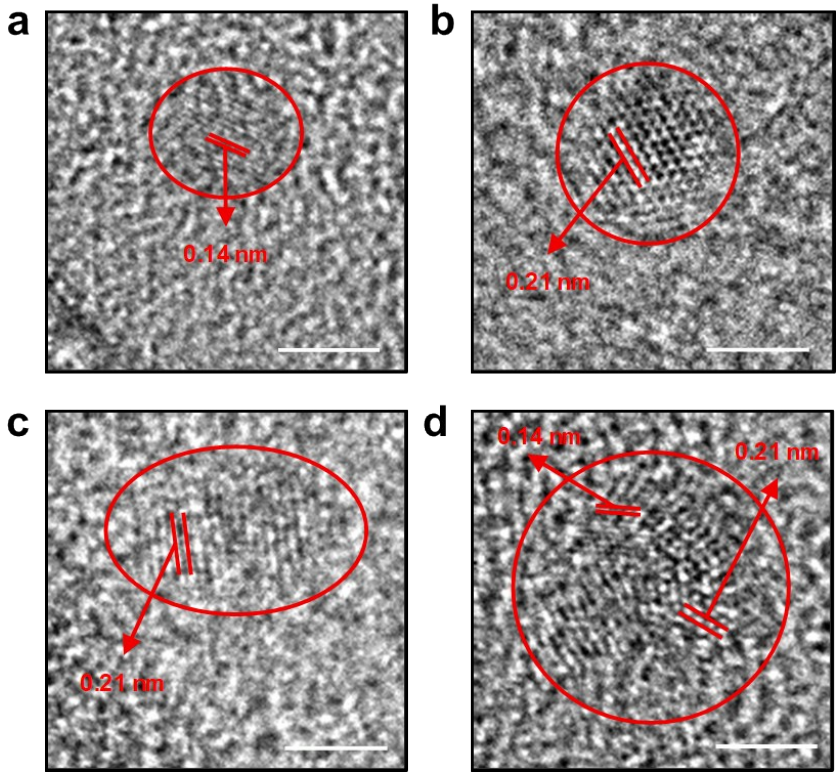

Fig. S8 HRTEM images of the R-CPDs at different heating durations of (a) 2 h, (b) 12 h, (c) 24 h and (d) 36 h.

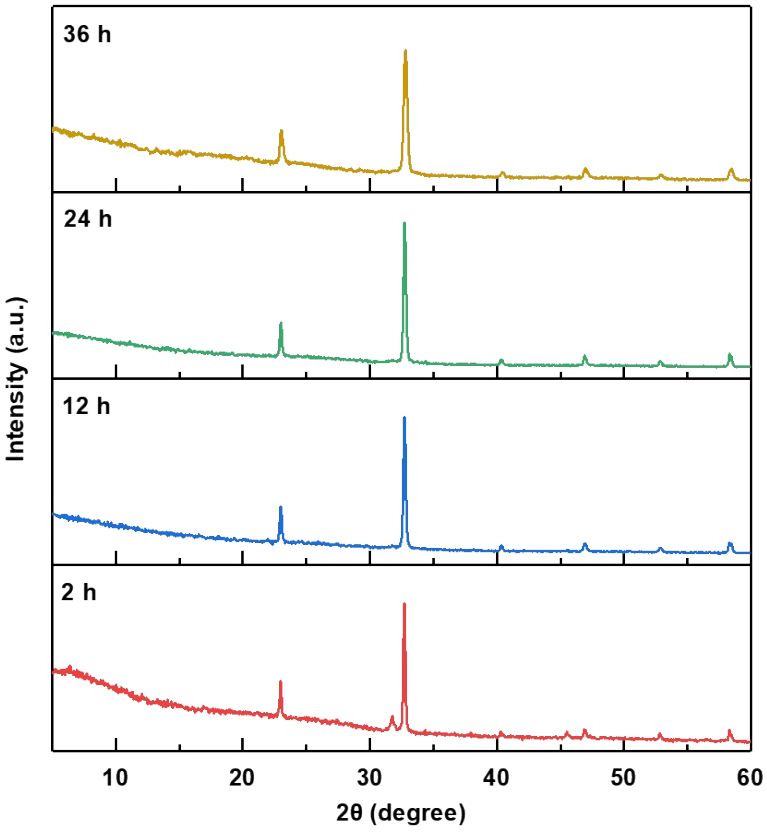

Fig. S9 XRD spectra of the R-CPDs at different heating durations.

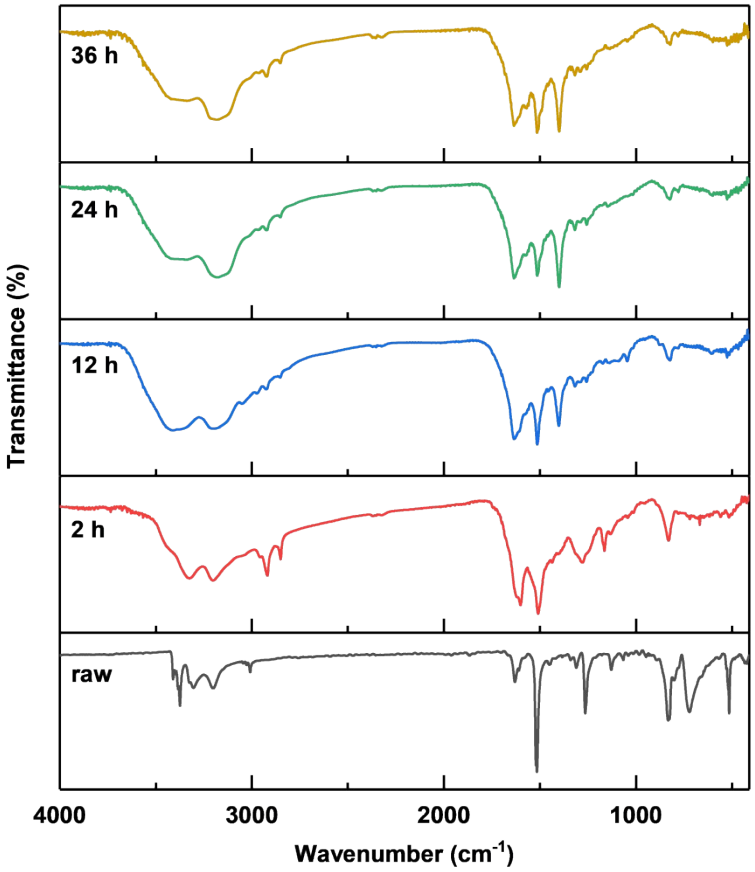

Fig. S10 FT-IR spectra of the raw material and the R-CPDs at different heating durations.

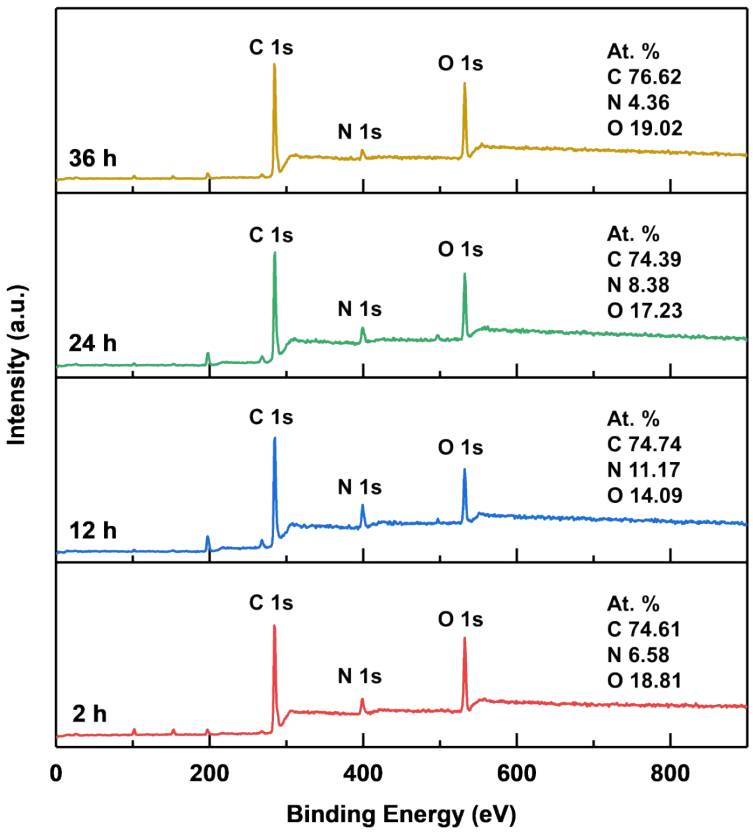

Fig. S11 XPS spectra of the R-CPDs at different heating durations.

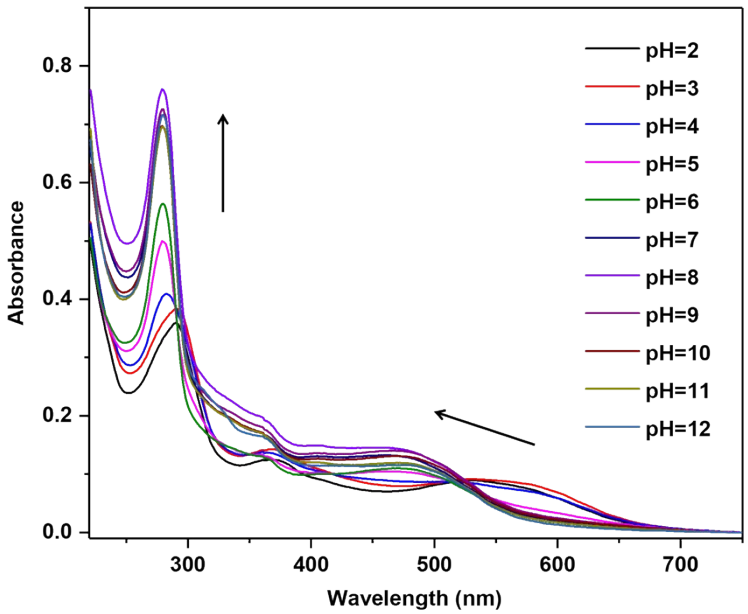

Fig. S12 UV-vis absorption spectra of the R-CPDs dispersed at different pH values (from 2 to 12). The R-CPDs used are obtained by heating reaction for 12 h.

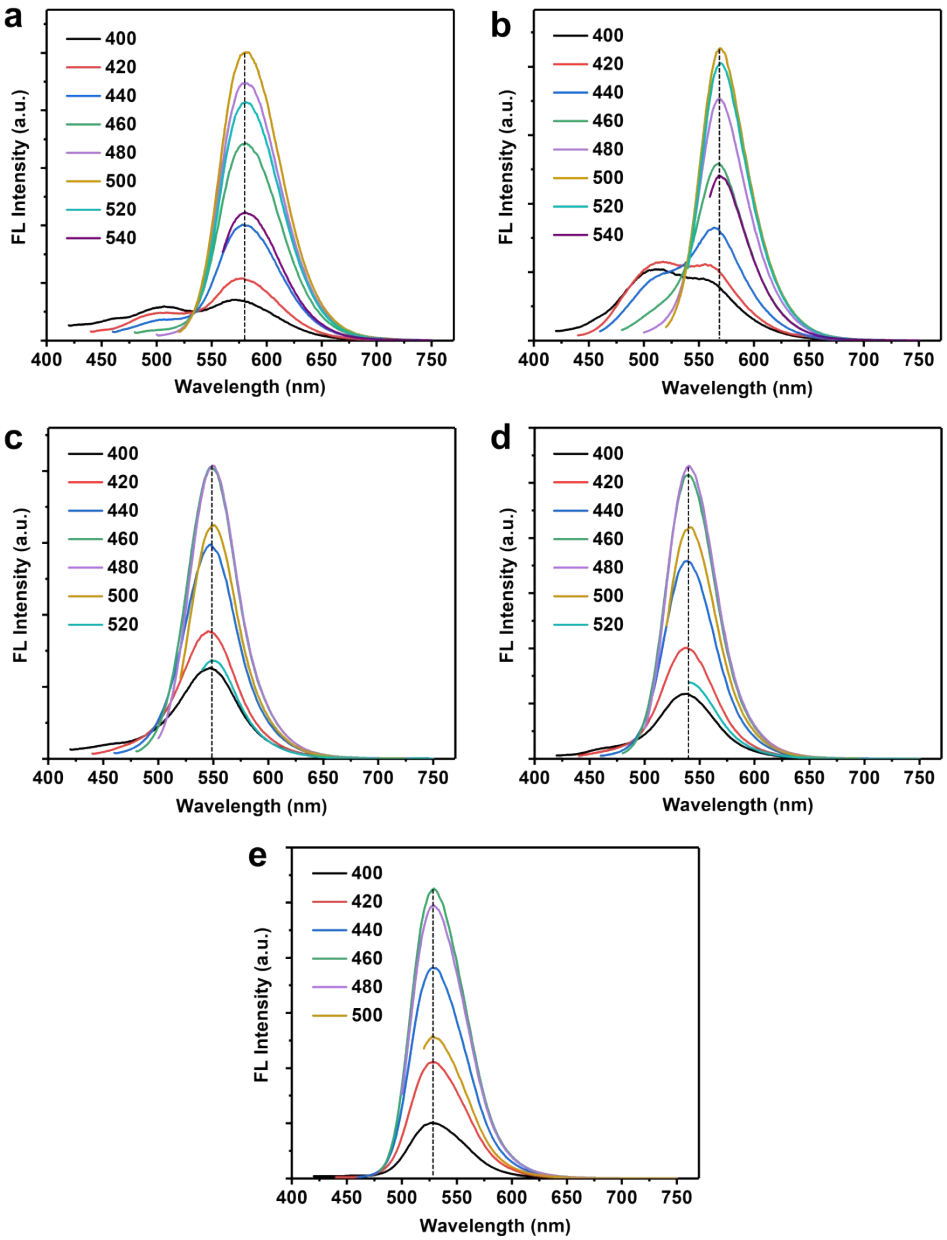

Fig. S13 FL spectra of the R-CPDs dispersed in (a) formamide, (b) dimethyl sulfoxide, (c) acetonitrile, (d) ethyl acetate and (e) methylbenzene under various excitation wavelengths. The R-CPDs used are obtained by heating reaction for 36 h.

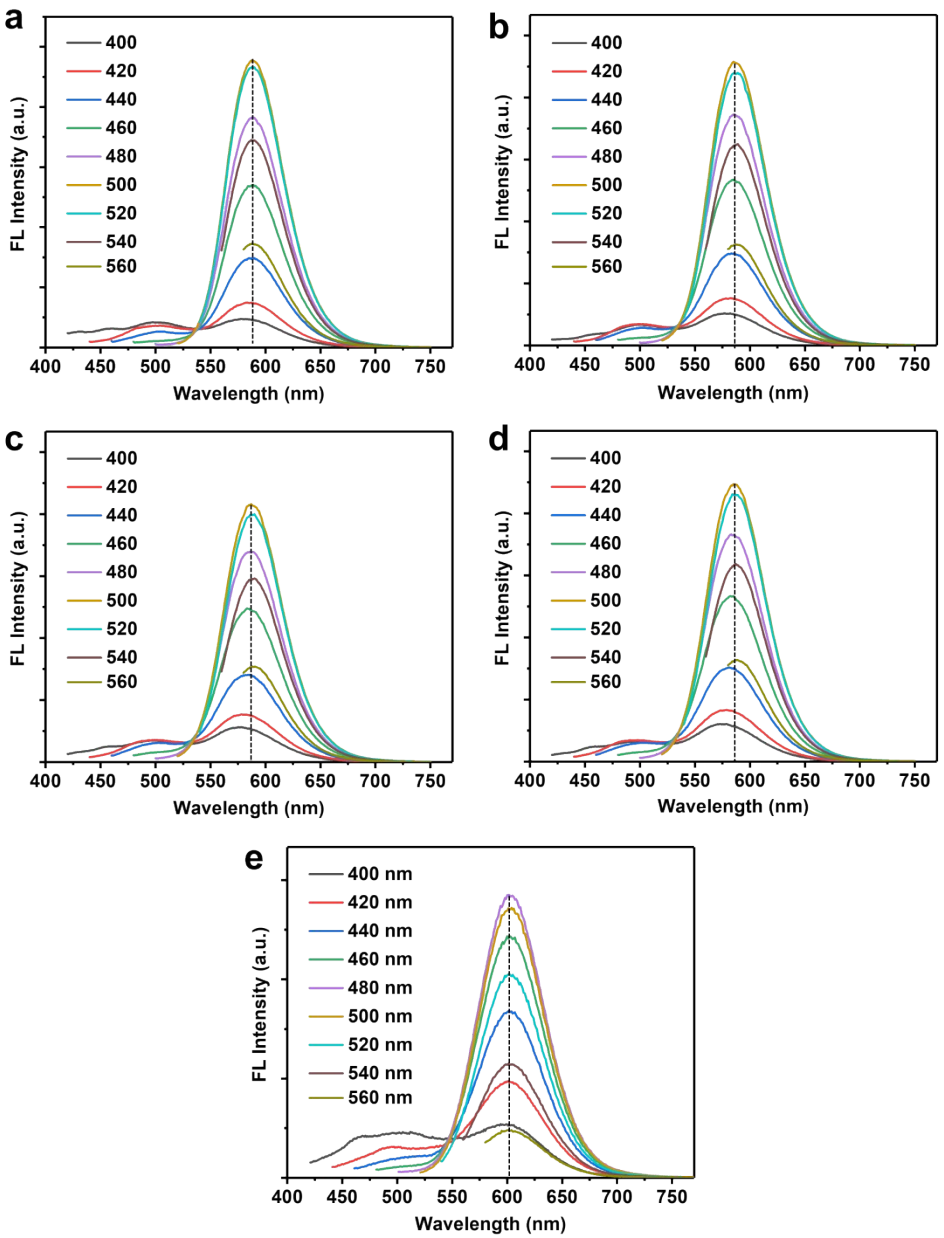

Fig. S14 FL spectra of the R-CPDs dispersed in (a) methanol, (b) ethanol, (c) 1-hexanol, (d) 1-octanol and (e) water under various excitation wavelengths. The R-CPDs used are obtained by heating reaction for 36 h.

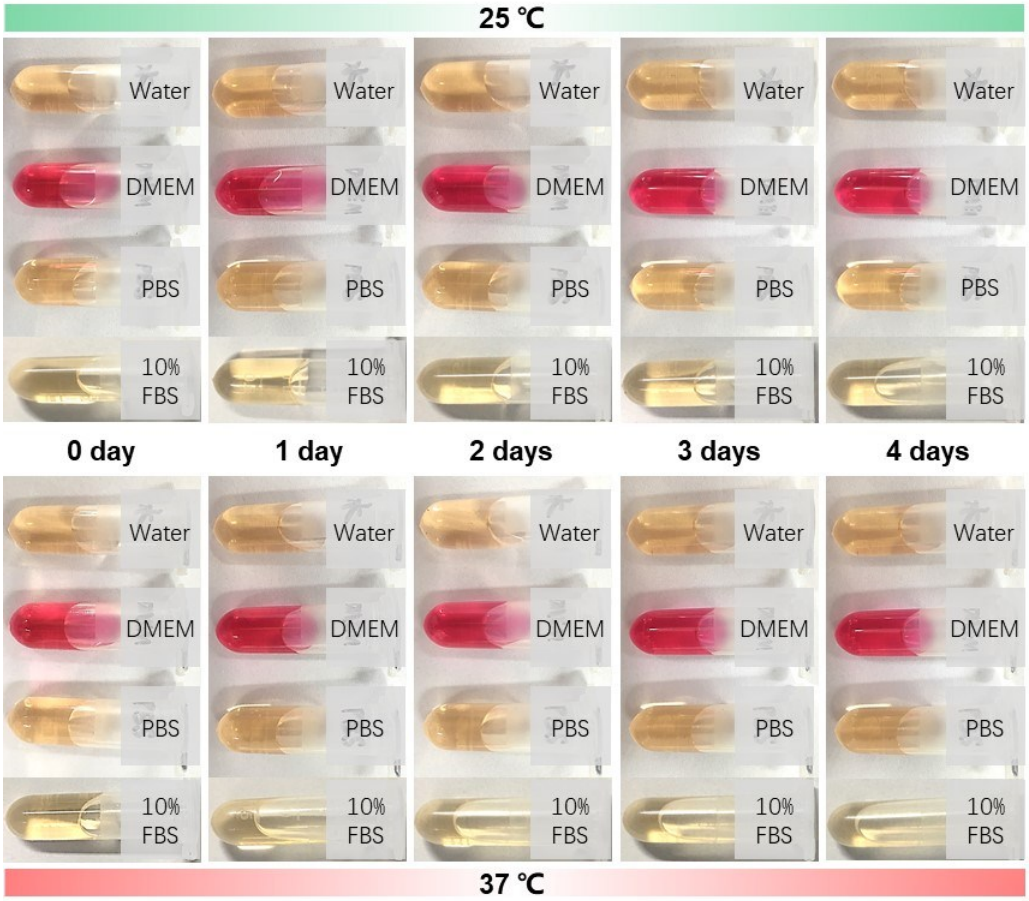

Fig. S15 Photographs of 100 μg mL^{-1} R-CPDs dispersed in physiological media at 25°C and 37°C for 4 days. The R-CPDs used are obtained by heating reaction for 12 h.

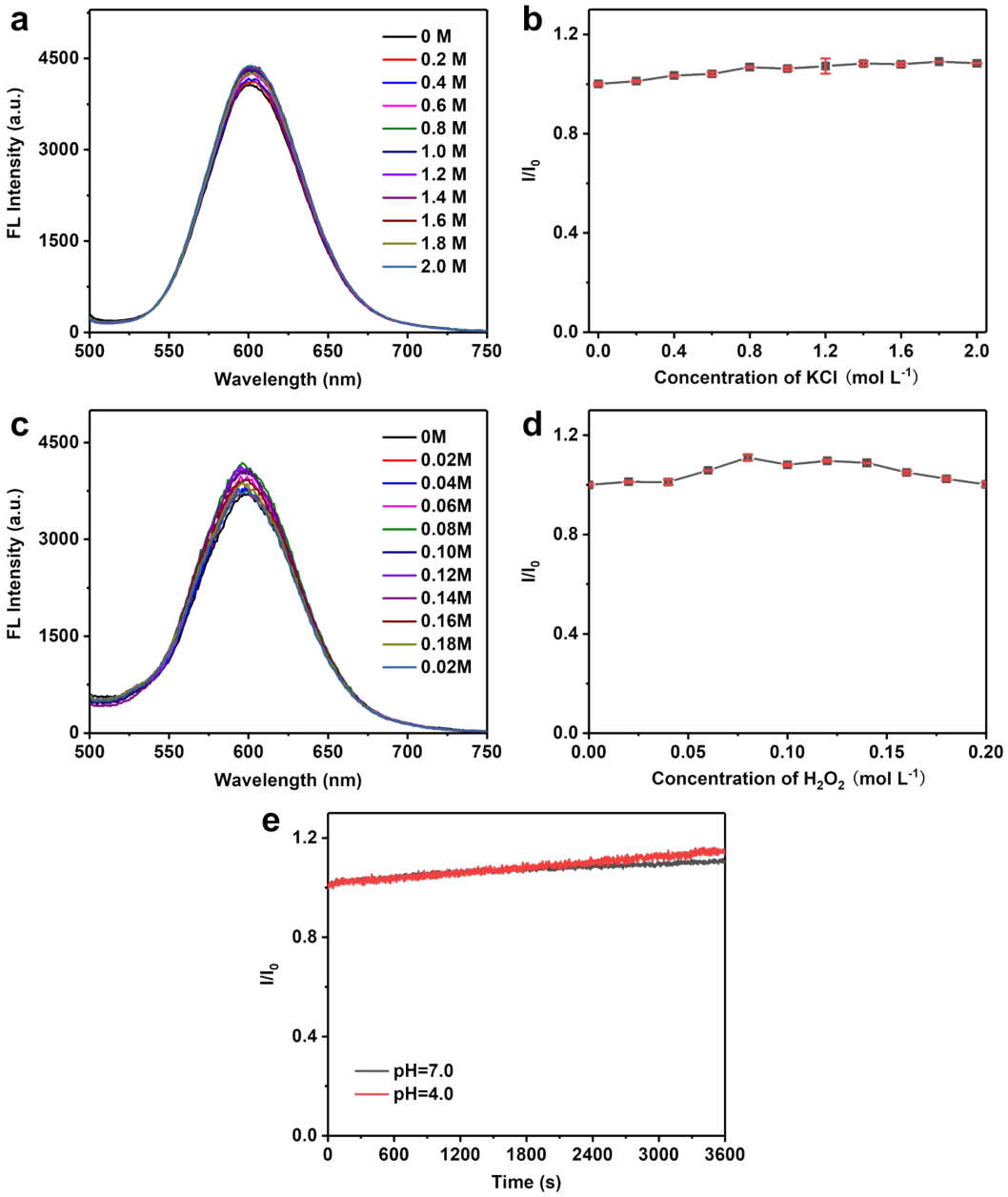

Fig. S16 The stability of the R-CPDs in a salty medium (a, b). The antioxidant capacity of the R-CPDs (c, d). The stability of the R-CPDs under irradiation of a 150 W Xe lamp. Conditions: $\lambda_{ex}/\lambda_{em}$= 480/600 nm. The R-CPDs used are obtained by heating reaction for 12 h.

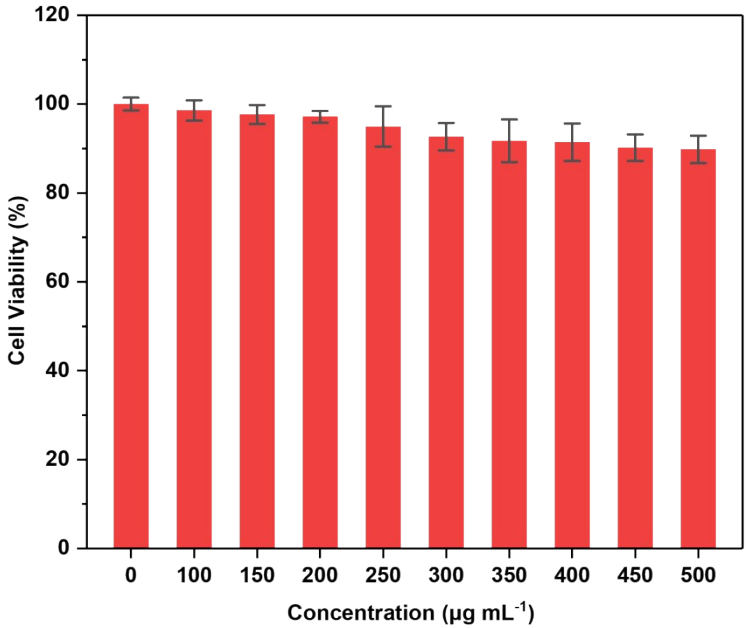

Fig. S17 Viability of HeLa cells after incubating with various concentrations of the R-CPDs for 24 h. The R-CPDs used are obtained by heating reaction for 12 h.

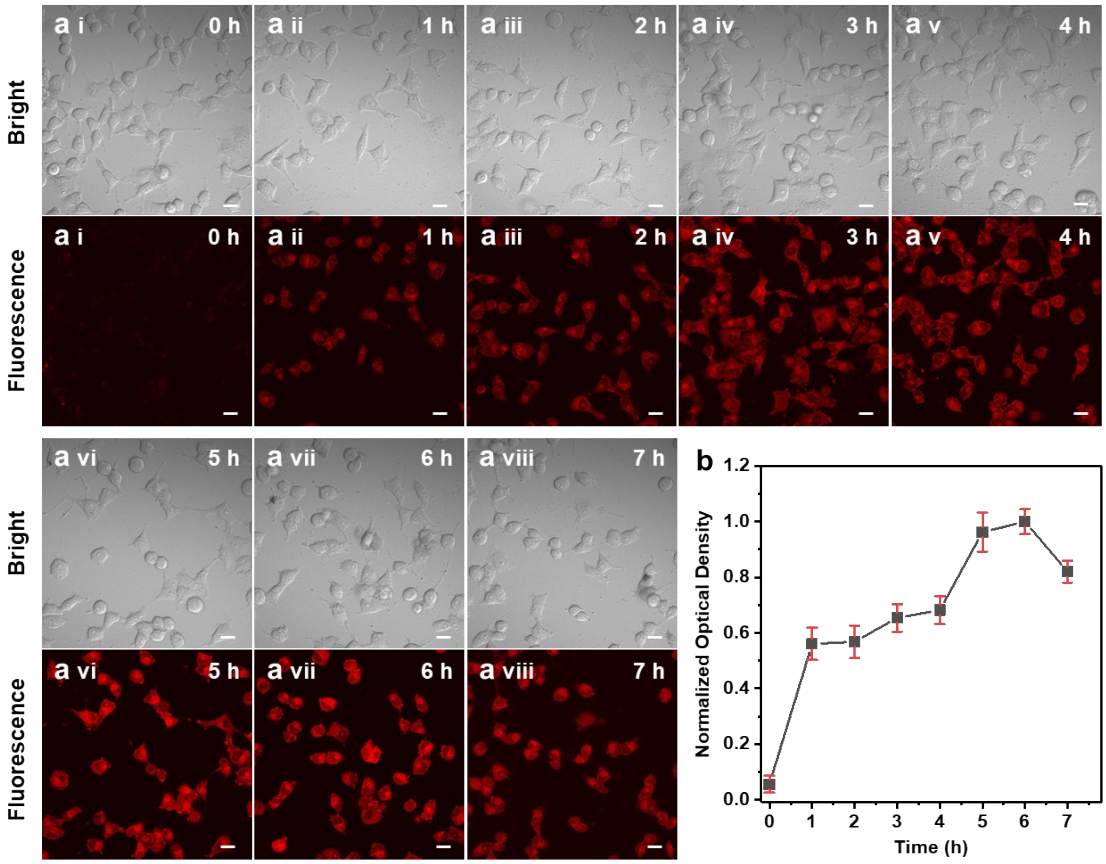

Fig. S18 (a) CLSM images of HeLa cells incubated with 100 μg mL^{-1} R-CPDs at different time-points (scale bar: 20 μm); (b) Plot of the normalized optical density of the R-CPDs-stained HeLa cells at different time-points. The R-CPDs used are obtained by heating reaction for 12 h.

Table S1 Comparison of typical pPD-derived long-wavelength fluorescent materials.

Material	Raw material	Preparation method	Diameter (nm)	Optical property ($\lambda_{ex}/\lambda_{em}$, QY)	Ref.
CNDs	pPD (ethanol)	Solvothermal reaction (180°C, in ethanol, 12 h); Silica column chromatography (methylene chloride, methanol).	10.0	510/603 nm, 26.1% (ethanol)	[1]
CQDs	pPD, urea	Hydrothermal reaction (160°C, 10 h); Silica column chromatography (ethyl acetate, ethanol).	2.6	521/625 nm, 23.81%	[2]
CNDs	pPD (ethanol)	Microwave-assisted reaction (800 W, in ethanol, 1 h (adding 1:1 water/ethanol)); Centrifugation (9000 rpm, 10 min); Silica column Chromatography (ethanol, ethyl acetate).	4	480/615 nm, 15%	[3]
CQDs	pPD (H_3PO_4)	Hydrothermal reaction (180°C, 24 h); Filtration; Neutralization; Centrifugation; Washing (ethanol, water).	2.4	530/622 nm, 11.2%	[4]
CQDs	pPD	Refluxing (250°C, diphenyl ether, 8 h); Precipitation (hexane); Centrifugation (4000 rpm, 20 min)	2.6	488/615 nm, 9.2%	[5]
Polymer	pPD (H_2O_2, catalyst)	Polymerization reaction (room temperature, in water, 24 h); Silica gel column chromatography (ethyl acetate, cyclohexane).	~24	512/638 nm, 0.01%	[6]
CPDs	pPD ($FeCl_3$)	Modulated polymerization (80°C, in water); Filtration (0.22 μm); Dialysis (vs. water).	1.7−3.3	480/600 nm, 6.7%	This work

Table S2 QYs of the R-CPDs at different heating durations.

Sample	Solvent	λ_{ex} (nm)	Φ_1 (%)	Φ_2 (%)	Φ_3 (%)	Φ_{ave} (%)
Rhodamine B	ethanol	480	55.4	55.3	55.3	55.3
R-CPDs (2 h)	water	480	0.2	0.1	0.2	0.2
R-CPDs (4 h)	water	480	4.8	4.4	5.0	4.7
R-CPDs (8 h)	water	480	6.2	6.2	6.6	6.3
R-CPDs (12 h)	water	480	7.0	6.4	6.6	6.7
R-CPDs (24 h)	water	480	5.6	5.4	5.2	5.4
R-CPDs (36 h)	water	480	4.1	4.2	4.0	4.1

Table S3 FT-IR analysis of the raw material and the R-CPDs at different heating durations.

Sample	Absorption peak (cm^{-1})	Group	Vibration mode
pPD	3202, 3009	N-H	stretching vibration
	1631, 1516	C=C	stretching vibration
	1264	N-H	in-plane bending vibration
	1129	C-H	in-plane bending vibration
	832	C-H	out-of-plane bending vibration
R-CPDs (2 h)	~3400-3600	O-H	stretching vibration
	~3200-3400	N-H	stretching vibration
	2919, 2850	C-H	stretching vibration
	1630	C=N/C=O	stretching vibration
	1601, 1510	C=C	stretching vibration
	1280	N-H	in-plane bending vibration
	1164	C-H	in-plane bending vibration
R-CPDs (12 h)	~3400-3600	O-H	stretching vibration
	~3200-3400	N-H	stretching vibration
	2926, 2853	C-H	stretching vibration
	1635	**C=N/C=O**	**stretching vibration**
	~1600, ~1570, 1515	C=C	stretching vibration
	1402	**C-N=**	**stretching vibration**
R-CPDs (24 h)	~3400-3600	O-H	stretching vibration
	~3180-3400	N-H	stretching vibration
	2923, 2851	C-H	stretching vibration
	1635	**C=N/C=O**	**stretching vibration**
	~1600, ~1570, 1517	C=C	stretching vibration
	1400	**C-N=**	**stretching vibration**
R-CPDs (36 h)	~3400-3600	O-H	stretching vibration
	~3180-3400	N-H	stretching vibration
	2924, 2852	C-H	stretching vibration
	1636	**C=N/C=O**	**stretching vibration**
	~1600, 1570, 1515	C=C	stretching vibration
	1400	**C-N=**	**stretching vibration**

Table S4 High-resolution C1s, N1s and O1s XPS spectra analysis of the R-CPDs at different heating durations.

Group	R-CPDs (2 h)	R-CPDs (12 h)	R-CPDs (24 h)	R-CPDs (36 h)
C-C/C=C	0.80	0.71	0.73	0.74
C-N/C-O	**0.11**	**0.23**	**0.19**	**0.17**
C=O/C=N	0.09	0.06	0.09	0.09
Pyridinic N	0.39	0.00	0.13	0.10
Amino N	0.39	0.62	0.46	0.58
Pyrrolic N	0.14	0.00	0.00	0.06
Graphitic N	**0.08**	**0.38**	**0.41**	**0.26**
C=O	0.63	0.37	0.60	0.57
C-O	0.37	0.63	0.40	0.43

References

1. K. Jiang, S. Sun, L. Zhang, Y. Lu, A. G. Wu, C. Z. Cai and H. W. Lin, *Angew. Chem., Int. Ed.*, 2015, **54**, 5360–5363.
2. H. Ding, S. B. Yu, J. S. Wei and H. M. Xiong, *ACS Nano*, 2016, **10**, 484–491.
3. C. X. Wang, K. L. Jiang, Q. Wu, J. P. Wu and C. Zhang, *Chem.-Eur. J.*, 2016, **22**, 14475–14479.
4. J. Chen, J. S. Wei, P. Zhang, X. Q. Niu, W. Zhao, Z. Y. Zhu, H. Ding and H. M. Xiong, *ACS Appl. Mater. Interfaces*, 2017, **9**, 18429–18433.
5. H. Wang, C. Sun, X. R. Chen, Y. Zhang, V. L. Colvin, Q. Rice, J. Seo, S. Y. Feng, S. N. Wang and W. W. Yu, *Nanoscale*, 2017, **9**, 1909–1915.
6. D. Rodriguez-Padron, A. D. Jodlowski, G. de Miguel, A. R. Puente-Santiago, A. M. Balu and R. Luque, *Green Chem.*, 2018, **20**, 225–229.